JOURNAL OF AGRICULTURAL AND FOOD CHEMISTRY

Agricultural and Environmental Chemistry

Design, Synthesis, Antibacterial Evaluation, and Induced Apoptotic Behaviors of Novel Epimeric and Chiral 18#-Glycyrrhetinic Acid Ester Derivatives with an Isopropanolamine Bridge against Phytopathogens

Meng Xiang, Xiang Zhou, Ting-Rong Luo, Peiyi Wang, Li-Wei Liu, Zhong Li, Zhibing Wu, and Song Yang

J. Agric. Food Chem., **Just Accepted Manuscript** • DOI: 10.1021/acs.jafc.9b06147 • Publication Date (Web): 08 Nov 2019

is published by the American Chemical Society. 1155 Sixteenth Street N.W., Washington, DC 20036

Design, Synthesis, Antibacterial Evaluation, and Induced Apoptotic Behaviors of Novel Epimeric and Chiral 18*β*-Glycyrrhetinic Acid Ester Derivatives with an Isopropanolamine Bridge against Phytopathogens

Meng Xiang [a], Xiang Zhou [a], Ting-Rong Luo [a], Pei-Yi Wang* [a], Li-Wei Liu [a], Zhong Li [b], Zhi-Bing Wu [a], Song Yang* [a,b]

[a] State Key Laboratory Breeding Base of Green Pesticide and Agricultural Bioengineering, Key Laboratory of Green Pesticide and Agricultural Bioengineering, Ministry of Education, Center for R&D of Fine Chemicals of Guizhou University, Guiyang, 550025, China.

[b] College of Pharmacy, East China University of Science & Technology, Shanghai, China 200237.

* Corresponding author.

E-mail: jhzx.msm@gmail.com (S. Yang), pywang888@126.com (P.-Y. Wang)

Abstract

Because only a handful of agrochemicals can manage bacterial infections, thus, the discovery and development of innovative, inexpensive, and high-efficiency antibacterial agents targeting these infections are challenging. Herein, a series of novel epimeric and chiral 18*β*-glycyrrhetinic acid (GA) ester derivatives with various tertiary amine pendants was designed, synthesized, and screened for pharmacological activity. Results showed that some of the title compounds were conferred with significantly enhanced antibacterial activity toward phytopathogens *Xanthomonas oryzae* pv. *oryzae* (**A$_2$**, **B$_1$**–**B$_3$**, and **C$_1$**, EC_{50} values within 3.81–4.82 μg/mL) and *Xanthomonas axonopodis* pv. *citri* (**B$_1$**, EC_{50} = 3.18 μg/mL; **B$_2$**, EC_{50} = 2.76 μg/mL). These activities are superior to those of GA (EC_{50} > 400 μg/mL), thiodiazole copper, and bismerthiazol. Pharmacophore studies revealed that the synergistic combination of GA skeleton and tertiary amine scaffolds contributed to the biological actions. *In vivo* experiments displayed their promising applications in controlling bacterial infections. Antibacterial mechanism studies revealed that the title compounds could trigger apoptosis in the tested pathogens, evident by bacteria morphological changes observed in scanning electron microscopy images. This outcome should motivate the development of various apoptosis inducers against plant bacterial diseases by a novel mode of action compared with existing agricultural chemicals.

Keywords

18*β*-glycyrrhetinic acid hybrids, antibacterial, *in vitro* and *in vivo* bioassays, apoptosis

45 **1. Introduction**

46 Plant bacterial diseases and induced complications represent a significant threat on
47 global food security and have become one of the greatest challenges in agriculture that
48 should be urgently addressed.[1-4] Currently, only a handful of agrochemicals, such as
49 thiodiazole copper (**TC**), bismerthiazol (**BT**), kocide, zhongshengmycin, streptomycin
50 (banned for its potential risk), and Zn thiazole, are used to manage these bacterial
51 diseases.[5,6] However, their limited field efficacies and the ever-increasing resistance
52 to these common pesticides have made crop protection a difficult task.[3,7-10] Therefore,
53 the discovery and development of innovative, inexpensive, low toxic, and
54 high-efficiency antibacterial agents targeting plant bacterial diseases have become the
55 primary task in agriculture.

56 Natural products are a valuable source that has long been exploited to treat
57 various diseases in medical and agricultural fields because of their wide range of
58 pharmacological behaviors.[11-16] As in the case of this study, natural products also
59 serve as major lead compounds for new drug development. Among these compounds,
60 pentacyclic triterpene ingredients found in many medicinal plants have been strongly
61 highlighted and extensively investigated for their substantial applications as flavor
62 sweeteners, food additives, cosmetics, substrate materials, and medical drugs.[17–20]
63 18*β*-Glycyrrhetinic acid (GA), a typical pentacyclic triterpenoid isolated from
64 *Glycyrrhiza* sp., has moderate hepatoprotective,[21-23] antioxidative,[24,25] antitumor,[26-28]
65 antipruritic,[29,30] and anti-inflammatory[31-33] effects. Moreover, it contains a natural
66 18-*β*-H-oleanane-type skeleton, a hydroxyl group at the C-3 position, an unsaturated

67 ketone at the C11–13 positions, and a carboxylic group at the C-20 position; thus, GA
68 contains ample functionality to serve as a lead compound.[27,34–36] However, GA has
69 some undesirable physicochemical features, including high hydrophobicity, which
70 contributes to its inadequate bioavailability, low water solubility and membrane
71 permeability, which seriously restrict its potential and practical applications.[37-39] To
72 enhance its water solubility, bioavailability, selectivity, and pharmacological effects,
73 numerous structural modifications based on the GA framework have been attempted,
74 resulting in abundant redecorated derivatives with broadened biological windows.[40-42]
75 Intensive investigations revealed that these modification strategies normally suffer
76 from a long or/and complicated synthetic route, usage of expensive reaction reagents,
77 and unsatisfactory biological effects. In contrast to these works, this study involved
78 the preparation of a series of simple epimeric and chiral GA derivatives with an ester
79 group and various tertiary amine pendants. These derivatives were prepared through
80 two facile substitution reactions to modulate the hydrophobicity of GA and explore
81 antibacterial agents targeting plant bacterial diseases. Within these title molecules, the
82 newly formed ester group and later introduced tertiary amines were used to potentially
83 improve biocompatibility and membrane penetrability, regulate molecular
84 hydrophobic/hydrophilic performances, promote binding affinity, and strengthen
85 additional interactions with target species. To our knowledge, few studies have used
86 this type of GA derivatization to evaluate the general antibacterial effect against plant
87 pathogens. In this study, phytopathogens *Xanthomonas oryzae* pv. *oryzae* (*Xoo*) and
88 *Xanthomonas axonopodis* pv. *citri* (*Xac*), which represent the most destructive

89 bacteria in agriculture, were tested.[43,44] The antibacterial mechanism was studied by
90 flow cytometry and scanning electron microscopy (SEM) after exposing the tested
91 pathogens to the designed drugs.

92 **2. Materials and methods**

93 **2.1 Instruments and Chemicals**

94 Bruker Biospin AG-400 (BRUKER OPTICS, Switzerland) and JEOLECX-500 NMR
95 (JEOL, Japan) spectrometers were used to confirm structural assignments of the
96 derivatives. $CDCl_3$ and TMS were used as the solvent and internal standard,
97 respectively. The related chemical shifts and coupling constants (*J*) were recorded in
98 parts per million (ppm) and hertz (Hz), respectively. Thermo Scientific Q Exactive
99 device (UItiMate 3000, Thermo SCIENTIFIC, United States) was exploited to detect
100 HRMS of title compounds dissolved in methanol. FEI Nova NanoSEM 450 (FEI,
101 United States) instrument was used for monitoring the morphology of tested
102 pathogens. The starting material 18β-glycyrrhetinic acid (purity > 97%) was
103 purchased from Energy Chemical of Saen Chemical Technology (Shanghai) Co., Ltd.

104 **2.2 Experimental section**

105 Turbidimeter test for *in vitro* antibacterial assay, *in vivo* testing for controlling rice
106 bacterial blight (compounds $\mathbf{B_1}$ and $\mathbf{C_1}$ were evaluated), and SEM patterns for tested
107 pathogens follow previously published protocols.[9]

108 **2.3 Apoptosis detection by flow cytometry**

109 The apoptotic effect triggered by $\mathbf{C_1}$ and $\mathbf{B_1}$ was evaluated by flow cytometry.
110 Meanwhile, the *Xoo* and *Xac* cells were double stained using AnnexinV-FITC and

propidium iodide (PI) under the guidance of the manufacturer's instruction (ANNEXIN V- FITC/PI Apoptosis Detection Kit, Solarbio). Briefly, *Xoo* (or *Xac*) was exposed to the related different concentrations of $\mathbf{C_1}$ ($\mathbf{B_1}$ was used for *Xac*) in nutrient broth medium (formula: 20 g glucose, 2 g yeast powders, 10 g peptone and 6 g beef extracts in 2.0 L deionized water) at 28 °C for 18 hours. Then 300 μL of bacteria liquid was took and incubated with 5 μL of annexin V-FITC for 10 min and 5 μL of PI for 5 min at room temperature in the dark. Samples were analyzed using a Gallios flow cytometer (BD Accuri C6).

3. Results and Discussion

The efficient preparation of GA ester derivatives is shown in Figure 2. In general, GA reacts with a racemic epibromohydrin in an *N*,*N*-dimethylformamide solution containing the base K_2CO_3 to yield the GA-ester **1** bearing the electrophilic epoxy tail. The epoxy tail was then ring-opened with a diverse set of secondary amines to provide an array of epimeric title compounds $\mathbf{A_1}$-$\mathbf{A_5}$, $\mathbf{B_1}$-$\mathbf{B_{10}}$, and $\mathbf{C_1}$-$\mathbf{C_{12}}$. Their final molecular frameworks were confirmed through analysis of their corresponding NMR and HRMS spectra. The *in vitro* toxicity of the designed compounds were analyzed by the classical turbidimetric test on the two plant bacterial strains *Xoo* and *Xac*. The bioactivity outcomes are illustrated in Table 1, which demonstrated that some of target compounds possess potent antibacterial capacity against these two plant pathogens with EC_{50} values of 3.81 and 2.76 μg/mL, respectively. Those data were substantially superior to those of GA (EC_{50} > 400 μg/mL), **BT**, and **TC**, indicating that this facile modification strategy on the GA framework could efficiently empower

133 these title compounds with desirable pharmacological effects. For series **A_1–A_5**,
134 slightly increasing the hydrophobic property of target compounds could lead to
135 improved antibacterial efficiency, as illustrated by comparing **A_1** (dimethyl, 10.5 and
136 9.57 μg/mL against *Xoo* and *Xac*, respectively) with **A_2** (diethyl, 3.81 and 5.10 μg/mL
137 against *Xoo* and *Xac*, respectively). By contrast, introducing the diallyl group (**A_3**),
138 diethanol group (**A_4**), or propargyl group (**A_5**) significantly quenched the antibacterial
139 effects. This finding indicated that a rigid and steric unsaturated alkane or a
140 hydrophilic hydroxyl pattern at the tail of the title compounds was disadvantageous to
141 bioactivity. When the above non-cyclic amines were modified into cyclic amines,
142 compounds **B_1–B_3** bearing pyrrolidine rings displayed significant inhibition toward
143 the tested pathogens, affording the corresponding EC_{50} values of 4.79, 4.15, and 4.43
144 μg/mL against *Xoo* and 3.18, 2.76, and 3.65 μg/mL against *Xac*. Increasing the ring
145 size to piperidine led to decreased bioactivity and yielded EC_{50} values within 6.89–
146 20.5 and 4.29–6.64 μg/mL for compounds **B_4–B_8** against *Xoo* and *Xac*, respectively.
147 Notably, the position of the methyl substituents on the piperidine ring showed ~3-fold
148 difference in anti-*Xoo* behavior, as demonstrated by comparing the EC_{50} values of
149 compounds **B_5** (2-CH_3, 10.7 μg/mL), **B_6** (3-CH_3, 7.19 μg/mL), and **B_7** (4-CH_3, 20.5
150 μg/mL), in which the methyl group at the 3-position was found to be beneficial to
151 anti-*Xoo* activity. Surprisingly, switching the methyl group (**B_6**) into ethyl formate
152 patterns (**B_9-B_{10}**) dramatically reduced antibacterial ability, suggesting that a
153 relatively bulk and/or dipole interactions from the ester group reduce activity. Further
154 modifying the piperidine moiety into various substituted piperazines afforded

155 different levels of antibacterial potency for compounds **C_1–C_{11}**. The anti-*Xoo* effect
156 was gradually reduced with the increment of carbon amounts (**C_1–C_5**) on the
157 piperazine ring and presented the minimal EC_{50} value of 4.82 μg/mL for **C_1**. Thus, an
158 additional hydrophobic and sterically hindered group was unfavorable to anti-*Xoo*
159 activity. Whereas less than a two-fold difference in activity was observed against *Xac*
160 with the same series of compounds. The introduction of an electron-withdrawing
161 group (acetyl, **C_6**) or substituted benzyl scaffolds (**C_7–C_{11}**) on the piperazine ring
162 failed to generate substantial bioactivity. Meanwhile, replacing the piperazine ring
163 into morpholine substructure (for compound **C_{12}**) provided negligible activity against
164 the two pathogens. This outcome showed that the nitrogen atom played a crucial role
165 in strengthening further interactions with the bacterial target species in contrast to the
166 oxygen atom. The bioassay results revealed that antibacterial functions were
167 influenced by diverse factors, including the type and size of amine and the
168 substituents on the *N*-containing scaffolds. Therefore, the molecular architectures
169 should be carefully optimized.

170 Compounds **B_1** (4.79 and 3.18 μg/mL) and **C_1** (4.82 and 3.66 μg/mL), which
171 possess excellent antibacterial competences, were selected as reference substances to
172 explore possible pharmacophores. Given the poor efficacy of GA, compound **D_1** was
173 primarily synthesized (Figure 3) to evaluate whether the bioactivity is ascribed to the
174 latter introduced motif containing an isopropanolamine bridge. However, **D_1** provided
175 weak antibacterial actions with the EC_{50} exceeding 100 μg/mL (Table 2). This
176 outcome indicated that the GA skeleton served as a vital ingredient in promoting the

177 pharmaceutical effects of final hybrids. Compounds **E_1** and **E_2** were prepared to
178 examine the influence of the introduced hydroxyl group in the compound A to C
179 series toward bioactivity (Figure 4). When the bioactivity of compound **B_1** was
180 compared, the removal of the hydroxyl group significantly reduced the antibacterial
181 power with EC_{50} values changing from 4.79 μg/mL (**B_1**, with hydroxyl group) to 53.7
182 μg/mL (**E_1**, without hydroxyl group) against *Xoo* and from 3.18 μg/mL (**B_1**) to 13.3
183 μg/mL (**E_1**) against *Xac*. An opposite pattern was obtained for **E_2** bearing the
184 piperazine group, which afforded improved potency against *Xoo* with an EC_{50} value
185 of 2.76 μg/mL and a similar effectiveness against *Xac* with an EC_{50} value of 3.17
186 μg/mL. This phenomenon indicated that this newly produced hydroxyl group could
187 affect the biological efficacy at different levels. Prudently, the absolute configuration
188 toward bioactivity should be investigated. Thus, compounds **F_1–F_4** were constructed
189 by switching the racemic reagents into the corresponding monomers. However,
190 anti-*Xoo* activity was reduced for these absolute single configurations, providing EC_{50}
191 values within 5.15–5.98 μg/mL. Differently, improved anti-*Xac* ability was observed
192 for **F_1–F_4**, affording EC_{50} values of 1.98–3.08 μg/mL. This interesting outcome
193 showed that the absolute configurations could weaken the interactive effects targeting
194 bacterial receptors of *Xoo* and heighten additional interactions with *Xac*. The above
195 investigations showed that the GA skeleton was essential for biological actions,
196 whereas the latter generated hydroxyl group and the absolute configuration could
197 influence bioactivity at varying degrees.

198 Bioactive compounds **B_1** and **C_1** bearing different types of *N*-containing

199 fragments were selected to detect potential *in vivo* effectiveness against rice bacterial
200 blight. The results showed that $\mathbf{B_1}$ and $\mathbf{C_1}$ exerted prominently therapeutic and
201 preventive effects at 200 μg/mL with control efficiencies within 50.19%–52.91%
202 (Table 3 and Figure 6). These values clearly outperformed those of commercial agents
203 (**BT** and **TC**, within 33.43%–42.39%), validating their potential applications as
204 antibiotic alternatives.

205 GA derivatives can induce apoptotic effects on tested cell lines including
206 SKOV3 and OVCAR3 cell lines, hepatocellular carcinoma cell lines, leukemia HL-60
207 cell lines, and A253 carcinoma cell lines.[27,45-49] Therefore, flow cytometry was
208 exploited to investigate the apoptotic actions of pathogens induced by the
209 corresponding bioactive compounds $\mathbf{C_1}$ (for *Xoo*) and $\mathbf{B_1}$ (for *Xac*). As revealed in
210 Figure 7, $\mathbf{C_1}$ could trigger remarkable late apoptotic behavior toward *Xoo* cells in a
211 dose-dependent manner, resulting in the percentage increasing from 14.2% (6.25
212 μg/mL, Figure 7b) to 87.7% (50 μg/mL, Figure 7e) for late apoptotic cells. This
213 interesting finding indicated that the anti-*Xoo* behavior of these novel GA hybrids
214 may be ascribed to the induced apoptotic mechanism of pathogens. Similarly, $\mathbf{B_1}$
215 could trigger the late apoptotic behavior of *Xac* with increased proportion from 6.5%
216 (6.25 μg/mL, Figure 8b) to 32.4% (50 μg/mL, Figure 8e). In addition, the ratio of
217 dead cells increased with increasing drug dosages, affording an increased percentage
218 of 15.4% at 25 μg/mL (Figure 8d). This intriguing outcome prompted us to further
219 explore the underlying antibacterial mechanism of GA hybrids. Such work may
220 benefit the development of various apoptosis inducers against plant bacterial diseases

221 by a novel mode of action compared with existing agricultural chemicals.

222 Topological studies on the pathogens treated with GA hybrids were conducted by
223 SEM frames in a dose-dependent way. As depicted in Figure 9, the outline of *Xoo* was
224 transformed from homogenous rod shapes (Figure 9a) to a mass of rods with
225 malformed surfaces (Figures 9b-9f). Furthermore, increase of drug concentrations led
226 to incrementally lysed or/and deformed cells, suggesting that strong interactions
227 occurred between the designed GA hybrids and pathogens. Similar events were
228 observed when *Xac* was treated with compound $\mathbf{B_1}$ (Figure 10), further verifying that
229 GA hybrids presented marked effects on the tested pathogens. This result was
230 consistent with the discovered apoptosis phenomenon.

231 In brief, several epimeric and chiral GA ester derivatives with diverse tertiary
232 amine pendants were synthesized and screened for antibacterial actions. The results
233 showed that certain title compounds were conferred with markedly enhanced
234 antibacterial behaviors toward the phytopathogens *Xoo* ($\mathbf{A_2}$, $\mathbf{B_1}$–$\mathbf{B_3}$ and $\mathbf{C_1}$, EC_{50}
235 values within 3.81–4.82 μg/mL) and *Xac* ($\mathbf{B_1}$, EC_{50} = 3.18 μg/mL; $\mathbf{B_2}$, EC_{50} = 2.76
236 μg/mL). This effect was superior to those of precursor GA (EC_{50} > 400 μg/mL), **TC**,
237 and **BT**. Pharmacophore studies revealed that the synergistic combination of the GA
238 skeleton and tertiary amine scaffolds dictated to the remarkable biological actions. *In*
239 *vivo* experimental results showed that $\mathbf{B_1}$ and $\mathbf{C_1}$ exerted prominent therapeutic and
240 preventive effects at 200 μg/mL with the control efficiencies in the range of 50.19%–
241 52.91%. These values clearly outperformed those of commercial agents (**BT** and **TC**,
242 within 33.43%–42.39%), validating their potential applications as antibiotic

alternatives. Antibacterial mechanism studies revealed that the title compounds could trigger the apoptosis of the tested pathogens, consequently resulting in changes in the bacterial morphology as observed in the SEM images. Given this facile structural modification and the promising biological behaviors, we anticipate that this study can provide a perceptible approach for modifying the GA framework to provide a series of antibacterial alternatives to current commercial agents.

Supporting Information

Supplementary data including synthesis, characterization data, ^{1}H NMR, ^{13}C NMR and ^{19}F NMR spectra for the intermediates and title compounds.

Funding Sources

We thank the Chinese government for support provided by grants NNSF (31860516, 21702037, 21877021, 21662009), Guizhou PSTP ([2012]6012, LH[2017]7259, [2017]5788), and Research Project of Ministry of Education (20135201110005, 213033A).

Conflict of interest

The authors declare no competing financial interest.

259 **Reference**

260 (1) Strange, R. N.; Scott, P. R. Plant disease: a threat to global food security. *Annu.*
261 *Rev. Phytopathol.* **2005**, *43*, 83-116.
262 (2) Chakraborty, S.; Newton, A. C. Climate change, plant diseases and food security:
263 an overview. *Plant Pathol.* **2011**, *60*, 2–14.
264 (3) Wang, P. Y.; Wang, M. W.; Zeng, D.; Xiang, M.; Rao, J. R.; Liu, Q. Q.; Liu, L.
265 W.; Wu, Z. B.; Li, Z.; Song, B. A.; Yang, S. Rational optimization and action
266 mechanism of novel imidazole (or imidazolium)-labeled 1,3,4-oxadiazole
267 thioethers as promising antibacterial agents against plant bacterial diseases. *J.*
268 *Agric*. *Food Chem*. **2019**, *67*, 3535-3545.
269 (4) Lo Cantore, P.; Iacobellis, N. S.; De Marco, A.; Capasso, F.; Senatore, F.
270 Antibacterial activity of *Coriandrum sativum* L. and *Foeniculum vulgare* Miller
271 Var. *vulgare* (Miller) essential oils. *J. Agric*. *Food Chem*. **2004**, *52*, 7862-7866.
272 (5) Wang, S. B.; Gan, X. H.; Wang, Y. J.; Li, S. Y.; Yi, C. F.; Chen, J. X.; He, F. C.;
273 Yang, Y. Y.; Hu, D. Y.; Song, B. A. Novel 1,3,4-oxadiazole derivatives
274 containing a cinnamic acid moiety as potential bactericide for rice bacterial
275 diseases. *Int. J. Mol. Sci.* **2019**, *20*, 1020.
276 (6) Li, P.; Hu, D. Y.; Xie, D. D.; Chen, J. X.; Jin, L. H.; Song, B. A. Design,
277 synthesis, and evaluation of new sulfone derivatives containing a
278 1,3,4-oxadiazole moiety as active antibacterial agents. *J. Agric. Food Chem.*
279 **2018**, *66*, 3093-3100.
280 (7) Chen, J. X.; Yi, C. F.; Wang, S. B.; Wu, S. K.; Li, S. Y.; Hu, D. Y.; Song, B. A.
281 Novel amide derivatives containing 1,3,4-thiadiazole moiety: Design, synthesis,
282 nematocidal and antibacterial activities. *Bioorg. Med. Chem. Lett.* **2019**, *29*,
283 1203-1210.
284 (8) Lin, Y. J.; He, Z. L.; Rosskopf, E. N.; Conn, K. L.; Powell, C. A.; Lazarovits, G.
285 A nylon membrane bag assay for determination of the effect of chemicals on
286 soilborne plant pathogens in soil. *Plant Dis*. **2010**, *94*, 201-206.
287 (9) Tao, Q. Q.; Liu, L. W.; Wang, P. Y.; Long, Q. S.; Zhao, Y. L.; Jin, L. H.; Xu, W.

M.; Chen, Y.; Li, Z.; Yang, S. Synthesis and in vitro and in vivo biological activity evaluation and quantitative proteome profiling of oxadiazoles bearing flexible heterocyclic patterns. *J. Agric. Food Chem.* **2019**, *67*, 7626-7639.

(10) Shuai, J. B.; Guan, F. Y.; He, B.; Hu, J. Q.; Li, Y.; He, D. H.; Hu, J. F. Self-assembled nanoparticles of symmetrical cationic peptide against citrus pathogenic bacteria. *J. Agric. Food Chem.* **2019**, *67*, 5720-5727.

(11) Camp, D.; Davis, R. A.; Campitelli, M.; Ebdon, J.; Quinn, R. J. Drug-like properties: guiding principles for the design of natural product libraries. *J. Nat. Prod.* **2012**, *75*, 72-81.

(12) Joo, Y. E. Natural product-derived drugs for the treatment of inflammatory bowel diseases. *Intest. Res.* **2014**, *12*, 103-109.

(13) Butler, M. S. Natural products to drugs: natural product derived compounds in clinical trials. *Nat. Prod. Rep.* **2005**, *22*, 162-195.

(14) Loiseleur, O. Natural products in the discovery of agrochemicals. *Chimia* **2017**, *71*, 810-822.

(15) Hüter, O. F. Use of natural products in the crop protection industry. *Phytochem. Rev.* **2010**, *10* , 185-194.

(16) Marrone, P. G. Pesticidal natural products-status and future potential. *Pest Manag. Sci.* **2019**, *75*, 2325-2340.

(17) Zhang, L. Y.; Dong, J. Z.; Liu, J.; Zhang, L. Y.; Kong, L. Y.; Yao, H. Q.; Sun, H. B. Synthesis and biological evaluation of novel pentacyclic triterpene derivatives as potential PPAR gamma agonists. *Med. Chem.* **2013**, *9*, 118-125.

(18) Xu, Q. M.; Liu, Y. L.; Feng, Y. L.; Tang, L. H.; Yang, S. L. A new E-ring gamma-lactone pentacyclic triterpene from Lysimachia clethroides and its cytotoxic activities. *Chem. Nat. Compd.* **2012**, *48*, 597-600.

(19) Huang, J. Y.; Yang, L. D.; Su, C. H.; Chu, X. W.; Zhang, J. Y.; Deng, S. P.; Cheng, K. G. Synthesis and cytotoxicity evaluation of pentacyclic triterpene–phenol nitrogen mustard conjugates. *Chem. Nat. Compd.* **2018**, *54*, 106-111.

(20) Jager, S.; Trojan, H.; Kopp, T.; Laszczyk, M. N.; Scheffler, A. Pentacyclic triterpene distribution in various plants-rich sources for a new group of

318 multi-potent plant extracts. *Molecules* **2009**, *14*, 2016-2031.
319 (21) Chen, H. J.; Kang, S. P.; Lee, I. J.; Lin, Y. L. Glycyrrhetinic acid suppressed
320 NF-kappaB activation in TNF-alpha-induced hepatocytes. *J. Agric. Food Chem.*
321 **2014**, *62*, 618-625.
322 (22) Wu, S. Y.; Cui, S. C.; Wang, L.; Zhang, Y. T.; Yan, X. X.; Lu, H. L.; Xing, G. Z.;
323 Ren, J.; Gong, L. K. 18beta-Glycyrrhetinic acid protects against
324 alpha-naphthylisothiocyanate-induced cholestasis through activation of the
325 Sirt1/FXR signaling pathway. *Acta Pharmacol. Sin.* **2018**, *39*, 1865-1873.
326 (23) Jeong, H. G.; You, H. J.; Park, S. J.; Moon, A. R.; Chung, Y. C.; Kang, S. K.;
327 Chun, H. K. Hepatoprotective effects of 18β-glycyrrhetinic acid on carbon
328 tetrachloride-induced liver injury: inhibition of cytochrome P450 2E1 expression.
329 *Pharmacol. Res.* **2002**, *46*, 221-227.
330 (24) Kong, S. Z.; Chen, H. M.; Yu, X. T.; Zhang, X.; Feng, X. X.; Kang, X. H.; Li, W.
331 J.; Huang, N.; Luo, H.; Su, Z. R. The protective effect of 18beta-Glycyrrhetinic
332 acid against UV irradiation induced photoaging in mice. *Exp. Gerontol.* **2015**, *61*,
333 147-155.
334 (25) Hosseinzadeh, H.; Nassiri-Asl, M. Pharmacological effects of glycyrrhiza spp.
335 and its bioactive constituents: update and review. *Phytother. Res.* **2015**, *29*,
336 1868-1886.
337 (26) Gao, C.; Dai, F. J.; Cui, H. W.; Peng, S. H.; He, Y.; Wang, X.; Yi, Z. F.; Qiu, W.
338 W. Synthesis of novel heterocyclic ring-fused 18beta-glycyrrhetinic acid
339 derivatives with antitumor and antimetastatic activity. *Chem. Biol. Drug Des.*
340 **2014**, *84*, 223-233
341 (27) Csuk, R.; Schwarz, S.; Siewert, B.; Kluge, R.; Strohl, D. Synthesis and antitumor
342 activity of ring A modified glycyrrhetinic acid derivatives. *Eur. J. Med. Chem.*
343 **2011**, *46*, 5356-5369.
344 (28) Zhang, L.; Yao, J.; Zhou, J. P.; Wang, T.; Zhang, Q. Glycyrrhetinic
345 acid-graft-hyaluronic acid conjugate as a carrier for synergistic targeted delivery
346 of antitumor drugs. *Int. J. Pharm.* **2013,** *441*, 654-664.
347 (29) Akasaka, Y.; Yoshida, T.; Tsukahara, M.; Hatta, A.; Inoue, H. Glycyrrhetinic

348 acid prevents cutaneous scratching behavior in mice elicited by substance P or
349 PAR-2 agonist. *Eur. J. Pharmacol.* **2011**, *670*, 175-179.
350 (30) Abramovits, W.; Perlmutter, A. Steroids versus other immune modulators in the
351 management of allergic dermatoses. *Curr. Opin. Allergy Cl.* **2006**, *6*, 345–354.
352 (31) Fan, B.; Jiang, B. C.; Yan, S. S.; Xu, B. H.; Huang, H. L.; Chen, G. T.
353 Anti-inflammatory 18beta-glycyrrhetinin acid derivatives produced by
354 biocatalysis. *Planta Med.* **2019**, *85*, 56-61.
355 (32) Radwan, M. O.; Ismail, M. A. H.; El-Mekkawy, S.; Ismail, N. S. M.; Hanna, A.
356 G. Synthesis and biological activity of new 18β-glycyrrhetinic acid derivatives.
357 *Arab. J. Chem.* **2016**, *9*, 390-399.
358 (33) Wu, C. H.; Chen, A. Z.; Yen, G. C. Protective effects of glycyrrhizic acid and
359 18beta-glycyrrhetinic acid against cisplatin-induced nephrotoxicity in BALB/c
360 mice. *J. Agric. Food Chem.* **2015**, *63*, 1200-1209.
361 (34) Hussain, H.; Green, I. R.; Shamraiz, U.; Saleem, M.; Badshah, A.; Abbas, G.;
362 Rehman, N. U.; Irshad, M. Therapeutic potential of glycyrrhetinic acids: a patent
363 review (2010-2017). *Expert Opin. Ther. Pat.* **2018**, *28*, 383-398.
364 (35) Gaware, R.; Khunt, R.; Czollner, L.; Stanetty, C.; Da Cunha, T.; Kratschmar, D.
365 V.; Odermatt, A.; Kosma, P.; Jordis, U.; Classen-Houben, D. Synthesis of new
366 glycyrrhetinic acid derived ring A azepanone, 29-urea and 29-hydroxamic acid
367 derivatives as selective 11beta-hydroxysteroid dehydrogenase 2 inhibitors.
368 *Bioorg. Med. Chem.* **2011**, *19*, 1866-1880.
369 (36) Wang, L. J.; Geng, C. A.; Ma, Y. B.; Huang, X. Y.; Luo, J.; Chen, H.; Zhang, X.
370 M.; Chen, J. J. Synthesis, biological evaluation and structure-activity
371 relationships of glycyrrhetinic acid derivatives as novel anti-hepatitis B virus
372 agents. *Bioorg. Med. Chem. Lett.* **2012**, *22*, 3473-3479.
373 (37) Tian, Q.; Wang, X. H.; Wang, W.; Zhang, C. N.; Wang, P.; Yuan, Z.
374 Self-assembly and liver targeting of sulfated chitosan nanoparticles functionalized
375 with glycyrrhetinic acid. *Nanomed. Nanotechnol.* **2012**, *8*, 870-879.
376 (38) Lei, Y. Y.; Kong, Y. D.; Sui, H.; Feng, J.; Zhu, R. Y.; Wang, W. P. Enhanced
377 oral bioavailability of glycyrrhetinic acid via nanocrystal formulation. *Drug*

378 *Deliv. Transl. Res.* **2016**, *6*, 519-525.
379 (39) Dai, L. H.; Li, J.; Yang, J. G.; Men, Y.; Zeng, Y.; Cai, Y.; Sun, Y. X. Enzymatic
380 synthesis of novel glycyrrhizic acid glucosides using a promiscuous bacillus
381 glycosyltransferase. *Catalysts* **2018**, *8*, 615.
382 (40) Abdel Bar, F. M.; Elimam, D. M.; Mira, A. S.; El-Senduny, F. F.; Badria, F. A.
383 Derivatization, molecular docking and in vitro acetylcholinesterase inhibitory
384 activity of glycyrrhizin as a selective anti-Alzheimer agent. *Nat. Prod. Res.* **2019**,
385 *33*, 2591-2599.
386 (41) Zhou, F.; Wu, G. R.; Cai, D. S.; Xu, B.; Yan, M. M.; Ma, T.; Guo, W. B.; Zhang,
387 W. X.; Huang, X. M.; Jia, X. H.; Yang, Y. Q.; Gao, F.; Wang, P. L.; Lei, H. M.
388 Synthesis and biological activity of glycyrrhetinic acid derivatives as antitumor
389 agents. *Eur. J. Med. Chem.* **2019**, *178*, 623-635.
390 (42) Alho, D. P. S.; Salvador, J. A. R.; Cascante, M.; Marin, S. Synthesis and
391 antiproliferative activity of novel A-ring cleaved glycyrrhetinic acid derivatives.
392 *Molecules* **2019**, *24*, 2938.
393 (43) Nozue, K.; Park, C. J.; Ronald, P. C. Quantitative measurements of *Xanthomonas*
394 *oryzae pv. oryzae* distribution in rice using fluorescent-labeling. *J. Plant Biol.*
395 **2011**, *54*, 269-274.
396 (44) Wang, X. B.; Yan, J. H.; Wang, M. Q.; Liu, M. H.; Zhang, J. P.; Chen, L. J; Xue,
397 W. Synthesis and three-dimensional quantitative structure-activity relationship
398 study of quinazoline derivatives containing a 1,3,4-oxadiazole moiety as efficient
399 inhibitors against *Xanthomonas axonopodis pv. citri. Mol. Divers.* **2018**, *22*,
400 791-802.
401 (45) Logashenko, E. B.; Salomatina, O. V.; Markov, A. V.; Korchagina, D. V.;
402 Salakhutdinov, N. F.; Tolstikov, G. A.; Vlassov, V. V.; Zenkova, M. A. Synthesis
403 and pro-apoptotic activity of novel glycyrrhetinic acid derivatives. *Chembiochem*
404 **2011**, *12*, 784-794.
405 (46) Chen, J.; Zhang, Z. Q.; Song, J.; Liu, Q. M.; Wang, C.; Huang, Z.; Chu, L.;
406 Liang, H. F.; Zhang, B. X.; Chen, X. P. 18beta-Glycyrrhetinic-acid-mediated
407 unfolded protein response induces autophagy and apoptosis in hepatocellular

408 carcinoma. *Sci. Rep.* **2018**, *8*, 9365.
409 (47) Liu, D.; Song, D. D.; Guo, G.; Wang, R.; Lv, J. L.; Jing, Y. K.; Zhao, L. X. The
410 synthesis of 18beta-glycyrrhetinic acid derivatives which have increased
411 antiproliferative and apoptotic effects in leukemia cells. *Bioorg. Med. Chem.*
412 **2007**, *15*, 5432-5439.
413 (48) Lee, C. S.; Yang, J. C.; Kim, Y. J.; Jang, E. R.; Kim, W.; Myung, S. C.
414 18beta-Glycyrrhetinic acid potentiates apoptotic effect of trichostatin A on human
415 epithelial ovarian carcinoma cell lines. *Eur. J. Pharmacol.* **2010**, *649*, 354-361.
416 (49) Li, X. J.; Liu, Y. H.; Wang, N.; Liu, Y. Y.; Wang, S.; Wang, H. M.; Li, A. H.;
417 Ren, S. D. Synthesis and discovery of 18β-glycyrrhetinic acid derivatives
418 inhibiting cancer stem cell properties in ovarian cancer cells. *RSC Adv.* **2019**, *9*,
419 27294–27304.

420

421 **Figure captions**

422 **Figure 1.** Design strategy for 18*β*-glycyrrhetinic acid ester derivatives with various
423 tertiary amine pendants.

424 **Figure 2.** Synthetic route for $\mathbf{A_1}$–$\mathbf{A_5}$, $\mathbf{B_1}$–$\mathbf{B_{10}}$, and $\mathbf{C_1}$–$\mathbf{C_{12}}$.

425 **Figure 3.** Molecular structure for the control molecule $\mathbf{D_1}$.

426 **Figure 4.** Synthetic route for $\mathbf{E_1}$–$\mathbf{E_2}$.

427 **Figure 5.** Synthetic route for $\mathbf{F_1}$–$\mathbf{F_4}$.

428 **Figure 6.** *In vivo* experimental images of $\mathbf{B_1}$ and $\mathbf{C_1}$ against rice bacterial blight (drug
429 dosage: 200 μg/mL). **BT** and **TC** served as the positive comparison.

430 **Figure 7.** Apoptosis effect of *Xoo* monitored by flow cytometry after incubation with
431 escalating concentrations of $\mathbf{C_1}$. Cells were stained with annexin V-FITC and
432 propidium iodide (PI).

433 **Figure 8.** Apoptosis effect of *Xac* monitored by flow cytometry after treatment with
434 escalating concentrations of $\mathbf{B_1}$. Cells were stained with annexin V-FITC and
435 propidium iodide (PI).

436 **Figure 9.** Morphological changes in *Xoo* after treatment with escalating
437 concentrations of $\mathbf{C_1}$. Scale bars are 1 μm for a–f.

438 **Figure 10.** Morphological changes in *Xac* after treatment with escalating
439 concentrations of $\mathbf{B_1}$. Scale bars are 1 μm for a–f.

440 **Tables**

441 **Table 1.** *In vitro* antibacterial testing of **A_1–A_5**, **B_1–B_{10}**, and **C_1–C_{12}** against plant

442 bacterial strains *Xoo* and *Xac*.

Compounds	*Xoo*			*Xac*		
	Regression equation	R^2	EC_{50} (μg/mL)	Regression equation	R^2	EC_{50} (μg/mL)
GA			> 400			> 400
1			> 400			> 400
A_1	y=2.946x+1.987	0.979	10.5 ± 0.1	y=1.377x+3.649	0.976	9.57 ± 0.11
A_2	y=1.354x+4.214	0.969	**3.81 ± 0.18**	y=0.746x+4.472	0.997	5.10 ± 0.08
A_3			> 100			> 100
A_4			> 100			> 100
A_5			> 100			> 100
B_1	y=3.175x+2.839	0.981	**4.79 ± 0.08**	y=1.173x+4.410	0.999	**3.18 ± 0.02**
B_2	y=2.739x+3.307	0.995	**4.15 ± 0.11**	y=0.898x+4.604	0.999	**2.76 ± 0.16**
B_3	y=3.297x+2.868	0.988	**4.43 ± 0.08**	y=0.628x+4.647	0.944	3.65 ± 0.02
B_4	y=1.164x+4.024	0.973	6.89 ± 0.17	y=1.184x+4.051	0.998	6.33 ± 0.28
B_5	y=3.166x+1.741	0.905	10.7 ± 0.1	y=0.961x+4.273	0.967	5.71 ± 0.21
B_6	y=1.247x+3.932	0.980	7.19 ± 0.49	y=0.705x+4.554	0.967	4.29 ± 0.12
B_7	y=1.733x+2.726	0.984	20.5 ± 0.3	y=0.850x+4.462	0.957	4.30 ± 0.11
B_8	y=2.080x+2.564	0.998	14.8 ± 0.3	y=0.839x+4.310	0.979	6.64 ± 0.35
B_9			> 100			> 100
B_{10}			> 100			> 100
C_1	y=2.768x+3.109	0.960	**4.82 ± 0.08**	y=1.223x+4.311	0.894	3.66 ± 0.17
C_2	y=1.675x+3.571	0.934	7.13 ± 0.21	y=0.719x+4.579	0.956	3.85 ± 0.21
C_3	y=2.660x+2.372	0.915	9.73 ± 0.18	y=0.468x+4.736	0.999	3.67 ± 0.12
C_4	y=1.052x+3.361	0.954	36.1 ± 0.7	y=0.784x+4.519	0.999	4.11 ± 0.08
C_5	y=1.357x+2.936	0.967	33.2 ± 0.6	y=1.015x+4.152	0.894	6.85 ± 0.32
C_6			> 100			> 100
C_7			> 100			> 100
C_8			> 100			> 100
C_9			> 100			> 100
C_{10}			> 100			> 100
C_{11}			> 100			> 100
C_{12}			> 100			> 100
BT	y=1.499x+2.052	0.963	92.6 ± 2.1			
TC	y=1.540x+1.788	0.960	121.8 ± 3.6	y=2.153x+0.938	0.962	77.0 ± 2.0

443

444 **Table 2.** *In vitro* antibacterial testing of **D_1**, **E_1–E_2**, and **F_1–F_4** against plant bacterial

445 strains *Xoo* and *Xac*.

Compounds	*Xoo*			*Xac*		
	Regression equation	R^2	EC_{50} (μg/mL)	Regression equation	R^2	EC_{50} (μg/mL)
B_1	y=3.175x+2.839	0.981	**4.79 ± 0.08**	y=1.173x+4.410	0.999	**3.18 ± 0.02**
C_1	y=2.768x+3.109	0.960	**4.82 ± 0.08**	y=1.223x+4.311	0.894	3.66 ± 0.17
D_1			> 100			> 100
E_1	y=3.790x-1.556	0.995	53.7 ± 0.9	y=0.952x+3.930	0.974	13.3 ± 0.6
E_2	y=4.283x+3.110	0.998	**2.76 ± 0.06**	y=0.845x+4.576	0.998	**3.17 ± 0.11**
F_1 (*R*)	y=2.719x+3.047	0.999	5.23 ± 0.23	y=1.6155x+4.5148	0.947	**2.00 ± 0.03**
F_2 (*S*)	y=3.669x+2.149	0.944	5.98 ± 0.13	y=1.2163x+4.6381	0.886	**1.98 ± 0.07**
F_3 (*R*)	y=3.984x+1.992	0.998	5.69 ± 0.13	y=1.6148x+4.2118	0.932	**3.08 ± 0.11**
F_4 (*S*)	y=3.079x+2.808	0.844	5.15 ± 0.06	y=1.5889x+4.3551	0.992	**2.55 ± 0.03**
BT	y=1.499x+2.052	0.963	92.6 ± 2.1			
TC	y=1.540x+1.788	0.960	121.8 ± 3.6	y=2.153x+0.938	0.962	77.0 ± 2.0

446

447 **Table 3.** *In vivo* control efficiency (14 days after spraying) of $\mathbf{B_1}$ and $\mathbf{C_1}$ against rice

448 bacterial blight at 200 μg/mL.

Chemicals	Curative effect			Protective effect		
	Morbidity (%)	Disease index (%)	Control efficiency (%)[b]	Morbidity (%)	Disease index (%)	Control efficiency (%)[b]
B_1	100	40.46	51.83	100	40.44	51.85
C_1	100	41.83	50.19	100	39.56	52.91
BT	100	55.92	33.43	100	50.52	39.86
TC	100	48.39	42.39	100	52.86	37.07
CK[a]	100	84.00	/	100	84.00	/

449 [a] Negative control. [b] Statistical analysis was conducted by ANOVA under the condition of equal variances assumed ($P > 0.05$)

450 and equal variances not assumed ($P < 0.05$).

451 **Figures**

452 **Figure 1**

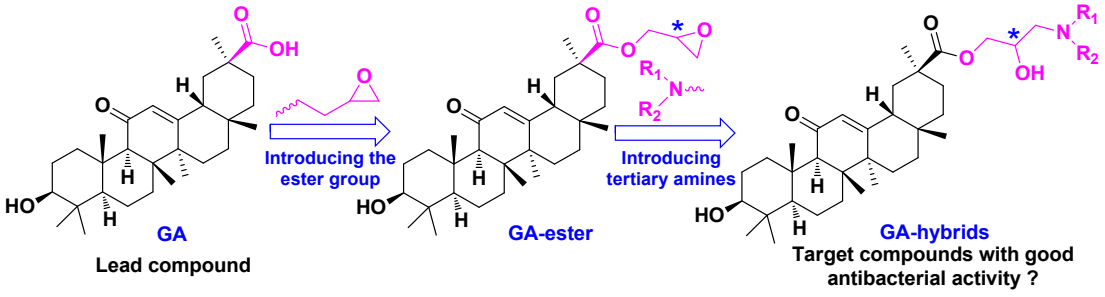

453

454 **Figure 2**

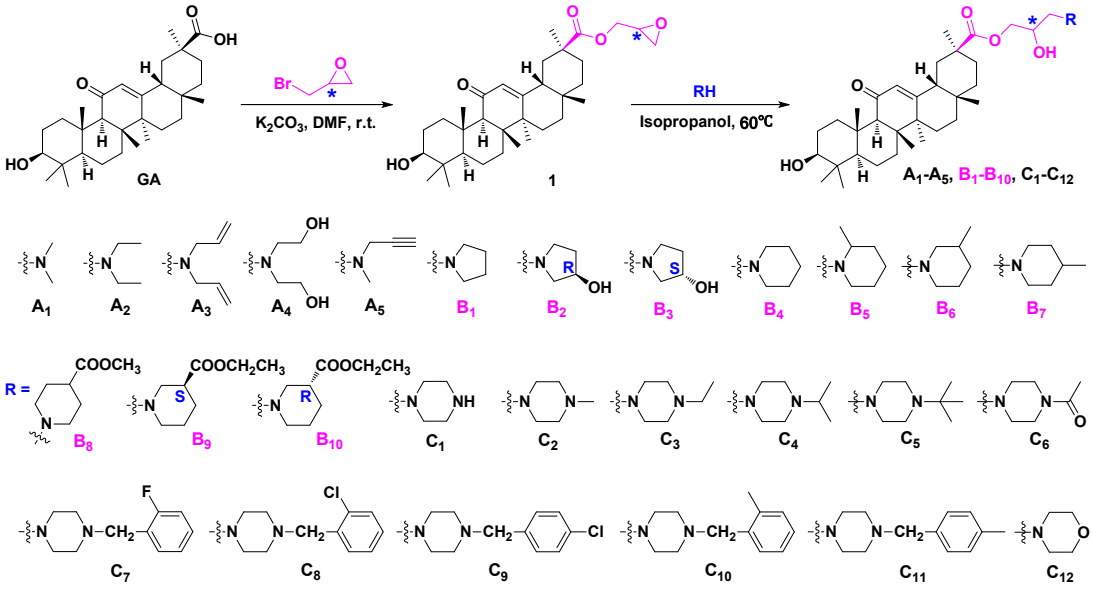

455

456 **Figure 3**

457

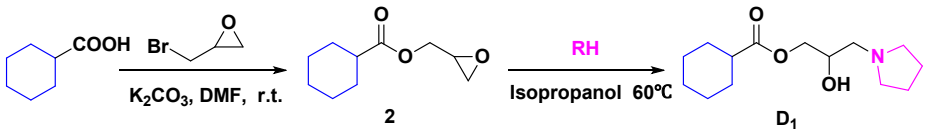

458 **Figure 4**

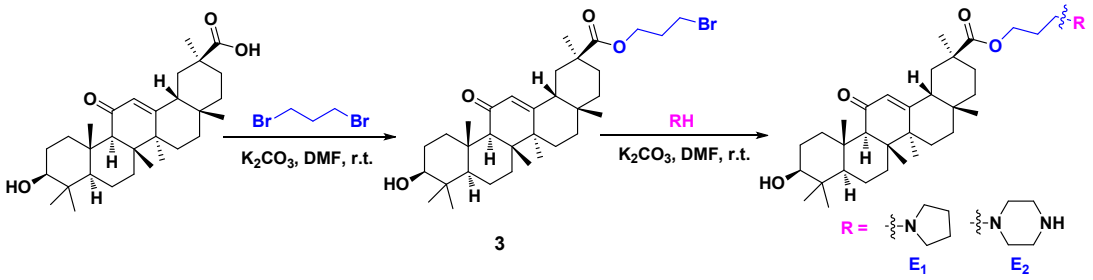

459

460 **Figure 5**

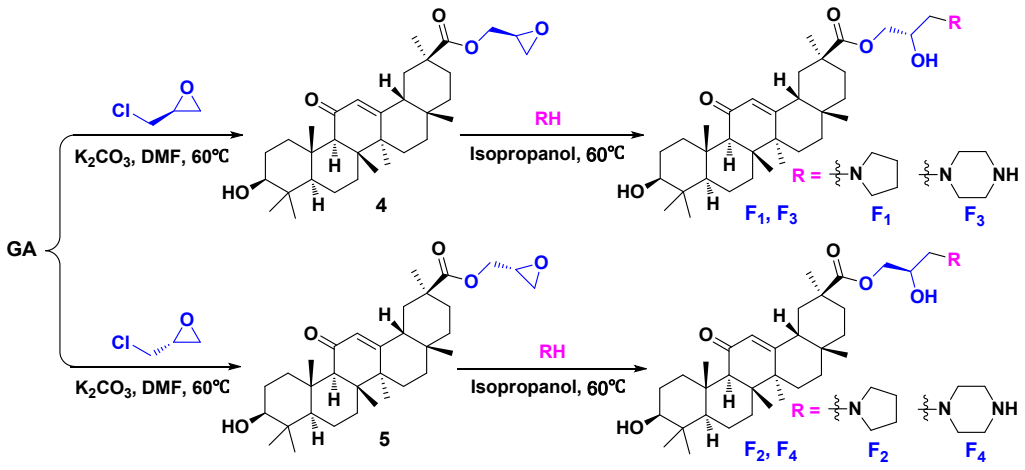

461

462 **Figure 6**

463

464

465 **Figure 7**

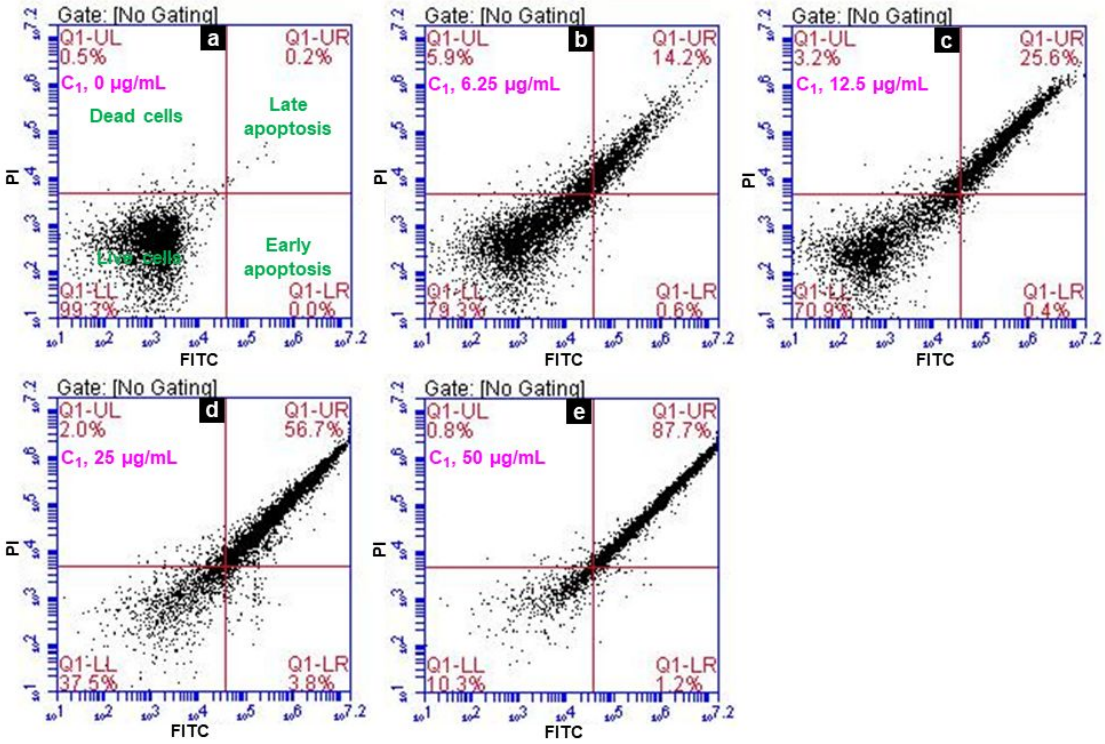

466

467 **Figure 8**

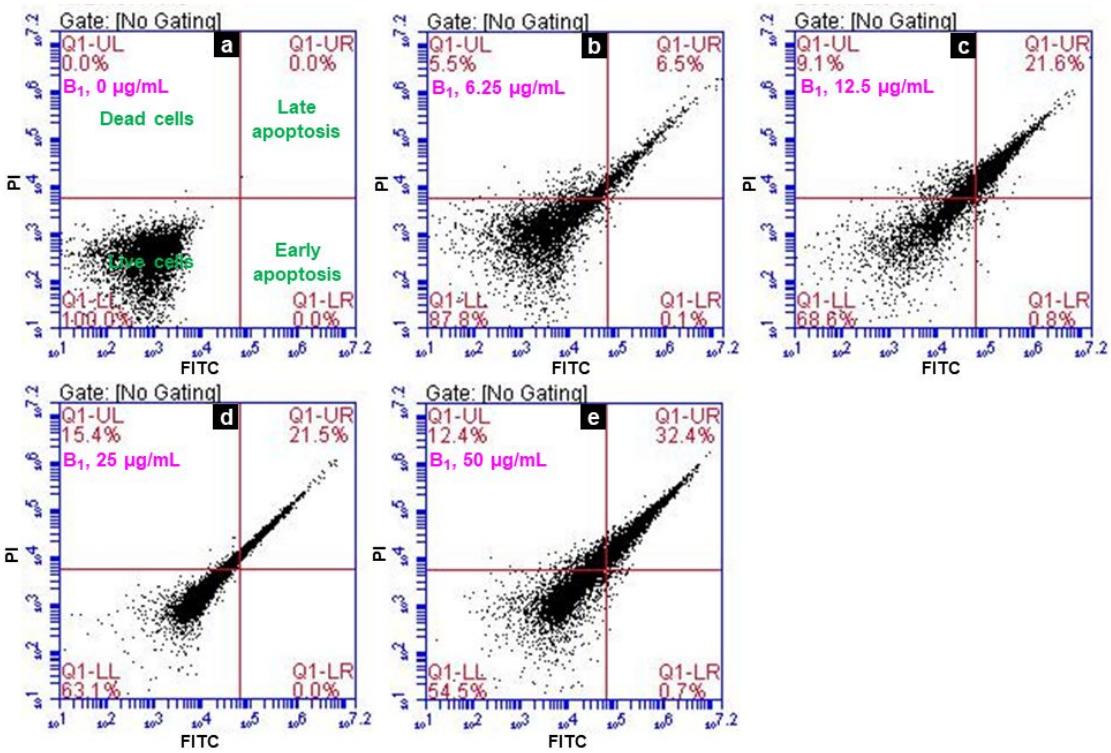

468

469 **Figure 9**

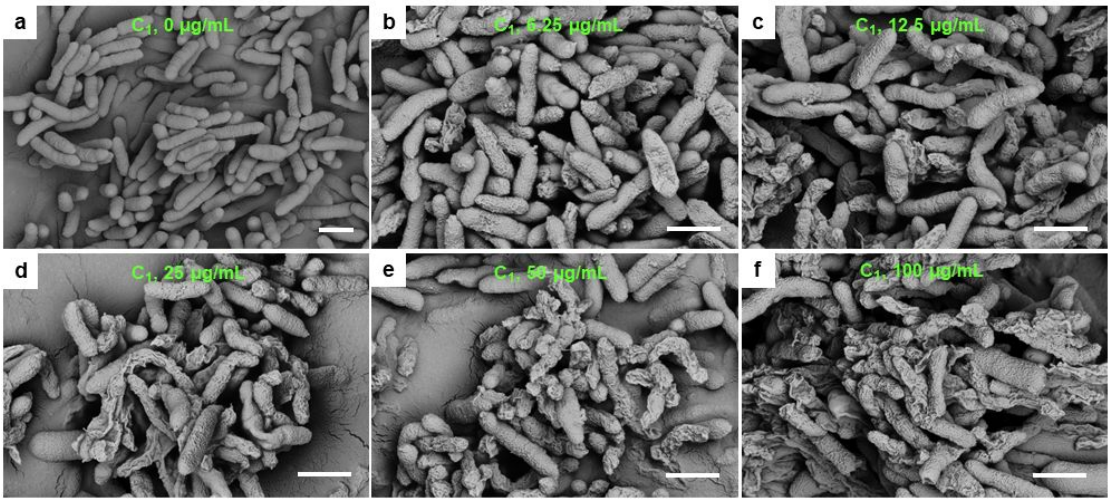

470

Figure 10

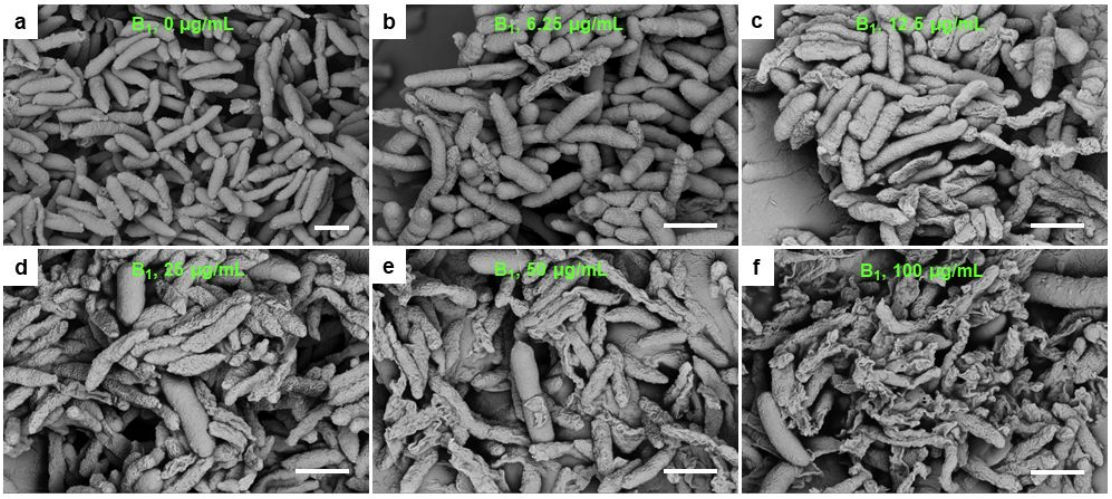
a
B_1, 0 μg/mL
b
B_1, 6.25 μg/mL
c
B_1, 12.5 μg/mL
d
B_1, 25 μg/mL
e
B_1, 50 μg/mL
f
B_1, 100 μg/mL

473 **Graphic for Table of Contents**

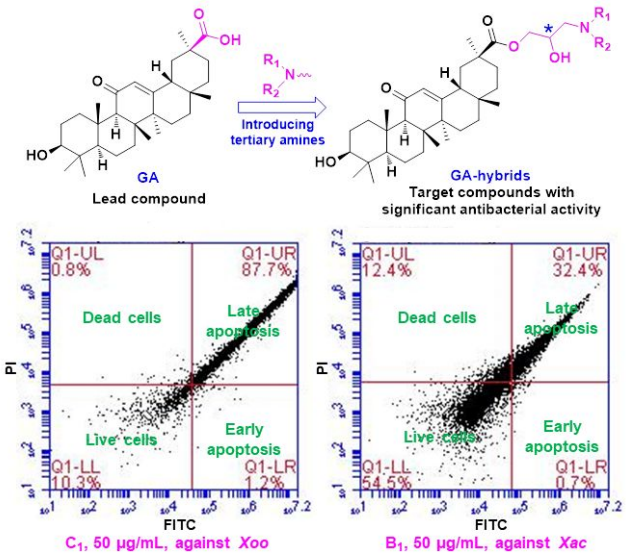

474